Shahrood University of Technology
Iranian Society of Mining Engineering (IRSME)
Journal of Mining and Environment (JME)
journal homepage: www.jme.shahroodut.ac.ir
THOMSON REUTERS

Application of Drone-Based Data for Directing Exploration Activities and Estimating Resources in Emperador Marble Quarry, Kerman Province, Iran

Hadi Shahriari[1]*, Mehdi Honarmand[2], Saeed Mirzaei[3] and Amir Saffari[4 and 5]

1- Department of Mining Engineering, Vali-e-Asr University of Rafsanjan, Rafsanjan, Iran
2- Department of Ecology, Institute of Science and High Technology and Environmental Sciences, Graduate University of Advanced Technology, Kerman, Iran
3- Department of Mining Engineering, Sarcheshmeh copper mine, National Iranian Copper Industries Co. (NICICo), Rafsanjan, Iran
4- Faculty of Mining, Petroleum & Geophysics Engineering, Shahrood University of Technology, Shahrood, Iran
5- Technical office, Eastern Alborz Coal Company, Shahrood, Iran

Article Info

Received 31 January 2022
Received in Revised form 20 February 2022
Accepted 24 February 2022
Published online 24 February 2022

DOI:10.22044/jme.2022.11616.2152

Keywords

Drone-based imagery
Photogrammetry
Marble quarry
3D deposit model
Block model

Abstract

This research work aims to discuss the methodology of using the drone-based data in the initial steps of the exploration program for the dimension stone deposits. A high-resolution imaging is performed by a low-cost commercial drone at the Emperador marble quarry, Kerman province, Iran. A ground resolution of 3 cm/pix is achieved by imaging at an altitude of 70 m in order to ensure the precise lithological and structural mapping. An accuracy of less than 5 cm is promised for the 3D photogrammetric products. Hence, the flight is performed with an 80% front and a 70% lateral image overlap. Furthermore, 18 ground control points (GCPs) are used in order to meet the required accuracy. Photogrammetric processing is done by the Agisoft PhotoScan software. The geology map is prepared through the visual geo-interpretation of the orthophoto image. The faults and fractures are delineated using the high-resolution orthophoto and hill-shade model in the ArcGIS software. Accordingly, the density map of fractures is produced, and the deposit is divided into five structural zones. The 3D deposit model with an accuracy of 2.8 cm is reconstructed based on the digital elevation model (DEM). A primary block model is generated using the 3D deposit model in the Datamine software in order to determine the resource for each structural zone. Finally, considering the amount of resource and situation of fractures, the priority of exploration for developing activities and appropriate methods is defined for each structural zone. The research work results have convinced us to include drone-based imagery in the initial steps of dimension stone exploration to consume the time and cost of the operation.

1. Introduction

Recent advances in the unmanned aerial system (UAS) technology and the development of photogrammetric processing methods have led to the increasing use of low-cost commercial drones in mining activities [1-4]. Reducing the operating costs, ease of use, and quick examination of an area have provided more opportunities for drones in order to participate in various parts of mining operations. This contribution covers almost all mining activities, from mineral exploration to mine closure and reclamation [5].

During the last decades, the remote sensing technology has served as an effective tool for mineral exploration using airborne and space-borne sensors. Now is the time to observe more contributions of remote sensing by offering the low-cost and high-quality UAV data in the reconnaissance and prospecting phases of mineral exploration campaigns. In the recent years, the drones equipped with spectral and geophysical instruments have been used for geological mapping and mineral exploration. Szentpeteril et al. [1] have utilized a quadcopter for pit mapping and 3D geological mapping in an open-cast mine in Malaysia. Blistan et al. [6] have conducted the lithological mapping of the inaccessible parts of a

Corresponding author: shahriarihi@gmail.com (H. Shahriari).

perlite mine in a mining area, Slovakia. Parvar et al. [7] have accomplished a magnetometry survey for localizing magnetic anomalies associated with host rocks of chromite mineralization in Oman. Malehmir et al. [8] have evaluated the potential of drone-based magnetometry for the exploration of iron ore deposits in central Sweden. Cunningham et al. [9] have identified a weak magnetic anomaly of a Zn deposit using the drone-based data in Canada. Kirsch et al. [2] have performed geological and hydrothermal alteration mapping using a drone equipped with hyperspectral sensors in Germany. Walter et al. [10] have compared the results of heliborne and drone-based magnetometry in the Shebandowan Greenstone Belt, Canada. This comparison indicated that the high-resolution magnetic data acquired by drones could aid in delineating the structural features related to gold mineralization. Dujoncquoy et al. [11] have applied the drone-based photogrammetric models for oil and gas exploration in Spain. Heincke et al. [12] have used hyperspectral imaging and magnetometry through multi-copter and fixed-wing platforms for geological and geophysical survey in Central Finland. The multi-copter system provided the data with a higher resolution, while the fixed-wing UAS surveyed the same area in a shorter time. Honarmand and Shahriari [13] have used the drone-based photogrammetric products for the exploration of vein-type Cu mineralization in Iran.

The limited flight time due to the capacity and weight of batteries has caused to use drones, especially of multirotor types, in the local-scale surveying objectives. Underexplored deposits and mines are appropriate places for drone imagery in order to handle issues in the field of monitoring mining activities, supervising safety conditions, expanding mineral exploration, etc. [2, 13, 14-18]. Drones provide accurate and high-resolution data for reconstructing the 3D geological models of deposits and up-dating geology data for continuously revising the in-used geological models of open-cast mines [1, 6, 11].

This research work aims to show the capability of drones for generating high-resolution products, managing the exploration activities, and estimating the resource of dimension stones in the first steps of mineral exploration campaigns. The Emperador marble quarry in the Kerman province, Iran, was selected as the case study. The rugged topography of the quarry has made difficulties for terrestrial mapping and developing fieldwork across the deposit. Drone-based imagery was thus used to facilitate geological and structural mapping. The technical aspects of aerial surveys are described. The method of deriving crucial information from the photogrammetric products is expressed. Finally, it is explained how to specify the exploratory zones and prioritize them based on the drone-based products.

2. Geology of studied area

The Sanandaj–Sirjan Zone (SSZ) is a metamorphic belt between the cities of Sirjan in the south-east and Sanandaj in the north-west of Iran (Figure 1). The metamorphism is related to the Zagros orogeny, and involves the metamorphic core of the Zagros continental collision zone in western Iran [19]. The lithology has been defined as the dominant rocks of Mesozoic age and Palaeozoic rocks, which rarely exhibit exposure in the south-east [19-20]. SSZ has been divided into two inner and outer belts [19]. The inner belt comprises mainly of Mesozoic metamorphic rocks. The outer belt of imbricate thrust slices involves the Zagros suture (radiolarite, Bisotun, ophiolite, and marginal sub-zones, which consist of Mesozoic deep-marine sediments, shallow-marine carbonates, oceanic crust, and volcanic arc, respectively). Another sub-division has been suggested by Eftekharnejad [21], who defined two sub-divisions, namely North SSZ and South SSZ, separated in the Golpaygan area. The south SSZ has been characterized by rock deformation in the Late Cretaceous. Furthermore, it was intruded by many felsic intrusive rocks. Rock deformation and metamorphism happened during the Middle to Late Triassic in the South SSZ [21-22]. Then SSZ was affected by an intense deformation until the end of the Cretaceous.

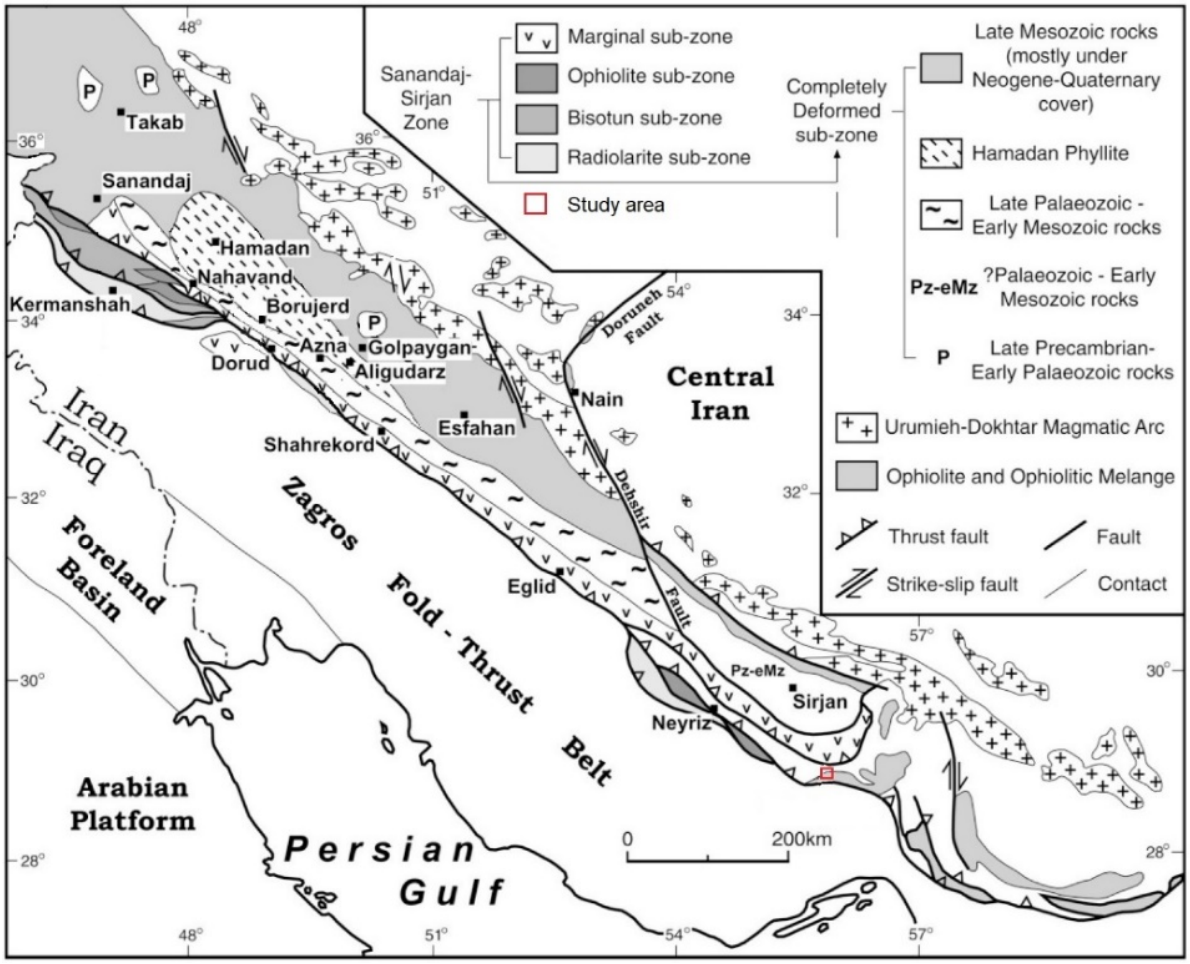

Figure 1. Simplified tectonic map of south-eastern Iran including Sanandaj-Sirjan zone [19].

The northwest-southeast trending SSZ includes several elongate sub-zones, namely complexly deformed, marginal, ophiolite, Bisotun, and radiolarite sub-zones [19]. The Emperador marble quarry, north-western of the Orzuieh geology map, is situated in the radiolarite sub-zone [23]. The radiolarite sub-zone involves the Triassic–Cretaceous limestone and dominant radiolarite. Figure 2 shows the location of the studied area in the north-western of the Orzuieh geology map. Based on the Orzuieh geology map, thin to medium bedded limestone, sandy and silty clay flat, and alluvial deposit are the dominant geological units.

Figure 3 presents the geology map of the Emperador marble quarry. The map was initially prepared based on the visual geo-interpretation of acquired images, and finalized after a geological survey. The geology is described as the Paleogene carbonate rocks and Quaternary alluvial deposits. Carbonate rocks experienced some degree of regional metamorphism. Dolomitic limestone is commonly seen in the Emperador quarry area.

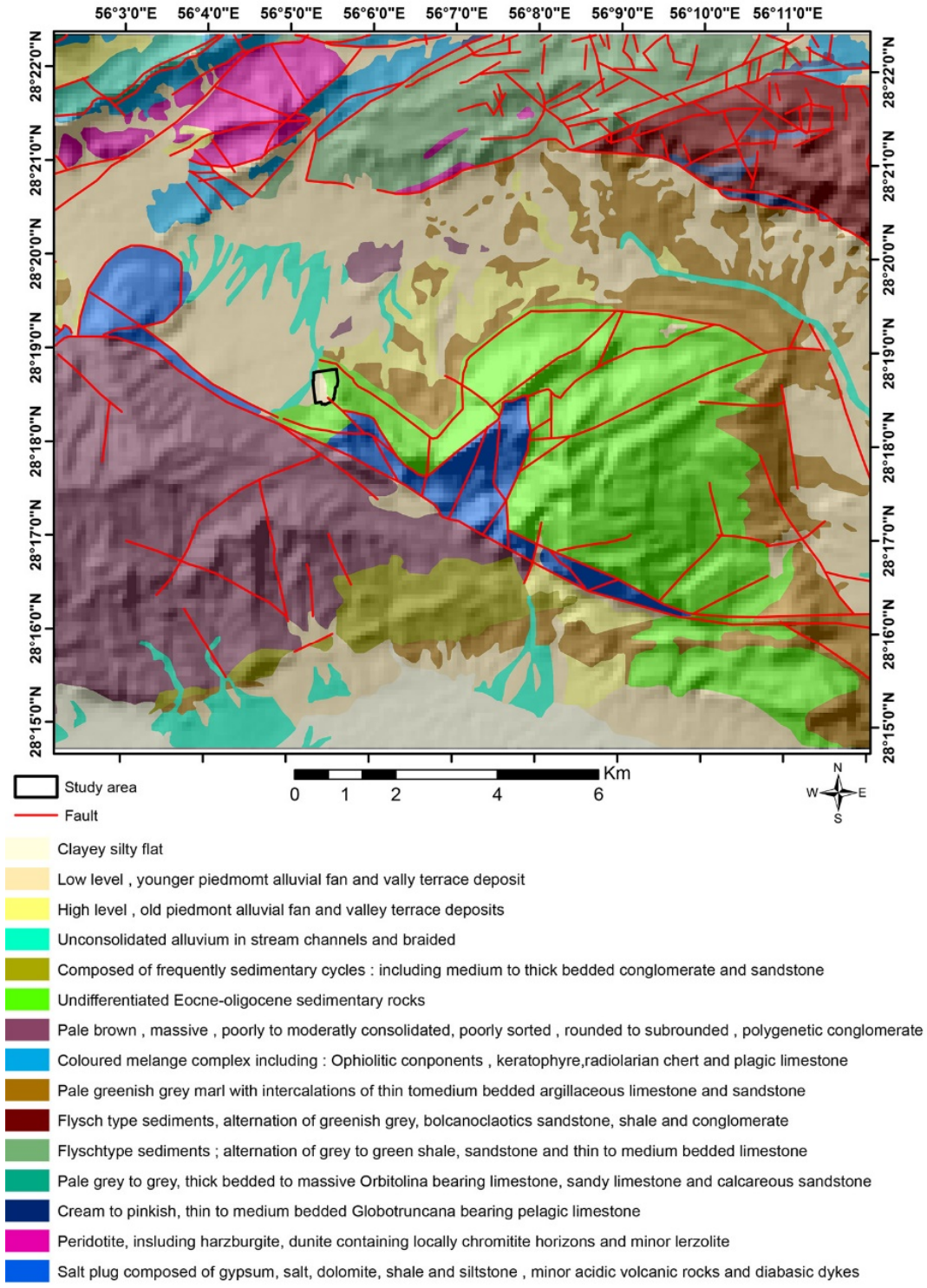

Figure 2. Regional geology map of studied area [23].

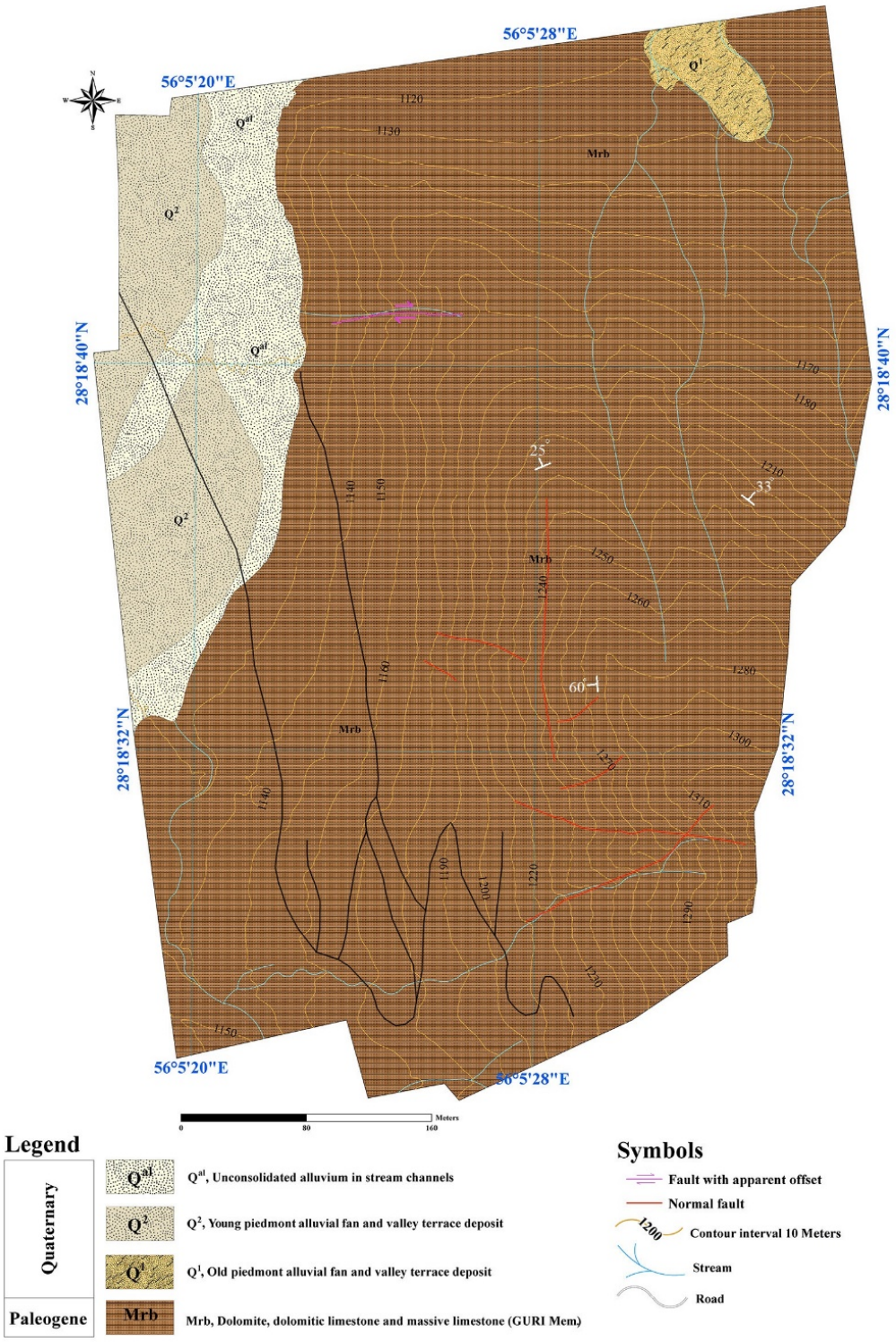

Figure 3. Geology map of studied area using drone-based photogrammetry.

The Emperador marble quarry has been opened using the diamond wire cutting method in one working bench (Figure 4a). Emperador marble is a kind of dark (or light) brown dolomitized limestone with white secondary calcite in the form of crystals and veins (Figures 4b and 4c). The mineralogical studies through the thin section and XRD introduced dolomite, calcite, and quartz as the main minerals (Figure 4d and 4e). No valuable metal or compound was delineated by XRF analysis.

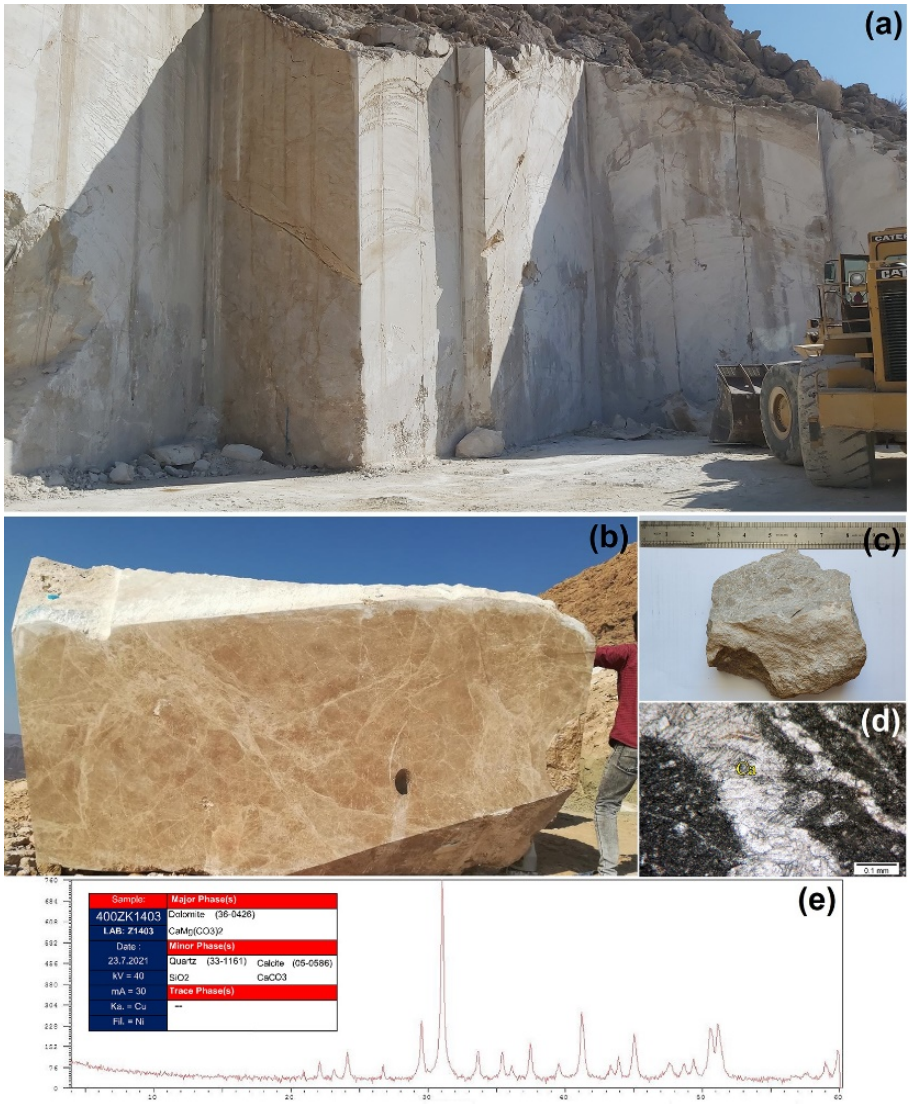

Figure 4. (a) Quarry face, (b) an extracted block and appearance of marble stone, (c) a hand specimen for mineralogical studies, and (d) a thin section (Ca: calcite), and (e) XRD result.

3. Material and Methods

In this research work, several types of 2D and 3D photogrammetric products were used in order to assist the primary evaluation of the Emperador marble quarry. The 2D products must ensure an appropriate ground resolution for extracting the geological boundary and structural features precisely. The 3D deposit models are a vital basis for the future mine plans that seek promised accuracy. Thus flight planning has an essential role in meeting the technical requirements of the project. The workflow of the research work is presented in Figure 5. Based on this figure, the photogrammetric products are used for creating different 2D and 3D products in order to assist the mineral exploration operations in the studied area.

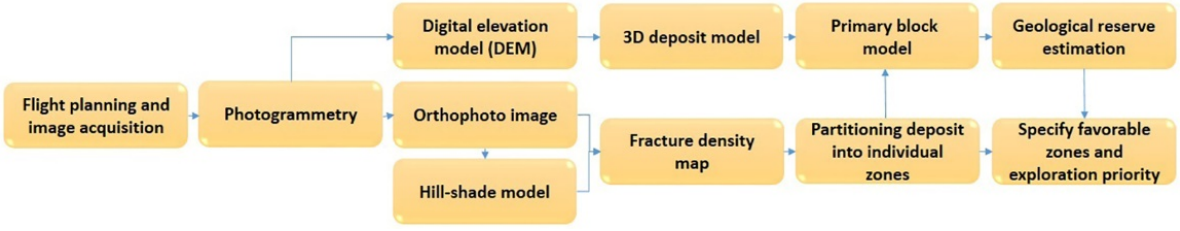

Figure 5. Workflow of research work.

3.1. Surveying plan and data acquisition

Image acquisition was conducted using a DJI Phantom 4 Pro V2.0. The platform is a lightweight commercial drone that has experienced successful missions in the geological studies [1, 2, 6, 11, 13, 24]. The drone carries a built-in CMOS camera on a stabilized gimbal. The camera captures high-resolution RGB images appropriate for the high-resolution imagery tasks such as geological and structural mapping [11, 13, 24].

In this research work, the geological and structural information was proposed to be derived from the photogrammetry products. The 3D models were developed for estimating the resource. Image acquisition is technically engaged with the flight parameters in order to ensure the desired quality of the 2D and 3D photogrammetric products. The spatial resolution and accuracy of products are two critical issues that are defined based on the project objectives, which are affected by flight settings.

Low altitude imagery results in an increase in the spatial resolution. However, it produces a larger volume of data, and consumes more operational time. Economically, low altitude imagery is applied on a local scale (e.g. deposit scale). Dai *et al*. [24] have evaluated the effect of drone altitude on the operational cost and spatial resolution. They accomplished geological mapping at a height of 50 m for the key areas using a DJI Phantom 4 Pro. Honarmand and Shahriari [13] have satisfied the geological and structural mapping with a flight height of 70 m by a DJI Phantom 4 Pro V2.0. They achieved a spatial resolution of 3.26 cm/pix for enhancing the geological boundaries and structural lineaments. In this work, the flight was performed at an altitude of 70 m. The spatial resolution of the CMOS camera was calculated using a binary (discrete) Siemens star target on a flat surface [13, 25-27].

The promised accuracy of the photogrammetry products was ensured by considering an appropriate image overlap and the use of ground control points (GCPs). The accuracy of the data acquired by non-RTK (real-time kinematic) drones is often improved using GCPs. The design of the flight path was performed in the DJIGo software. In order to achieve a total accuracy of less than 5 cm, the lateral and forward overlaps of 70% and 80% were, respectively, considered. This flight configuration was supported by a set of temporary GCPs in the shape of red crosses. The coordinate of GCPs was specified using a pair of SOUTH Galaxy G1+ receivers based on a ground-based real-time kinematic-differential global positioning system (RTK-DGPS). The evaluation of the overall accuracy was done using four check-points.

3.2. Photogrammetric processing

Photogrammetric processing provides a variety of products such as the high-resolution 2D raster images (orthomosaic or orthophoto), terrain models (digital surface models and digital terrain models), and 3D models (point clouds and mesh) [28]. The high-resolution orthophoto images are applied for deriving the features (e.g. lithological and structural mapping), while dense-point cloud model and DEM are used for the 3D modeling. In this research work, the photogrammetric processing was done using the Agisoft PhotoScan v1.4.4 software. A sparse-point cloud model was established using the acquired images and the camera positions file. The camera positions were optimized using the coordinates of GCPs in order to create an accurate dense-point cloud model [13, 18]. A mesh model was reconstructed based on the dense-point cloud, and was used for generating the orthophoto image. The geological features were extracted from the orthophoto images based on the visual interpretation in the ArcGIS 10.3 software. A hill-shade model was produced using the orthophoto image in the ArcGIS 10.3 software to help enhance the structural features.

3.3. 3D modeling and generating primary block model

Reconstructing the 3D models of the surficial deposits could help manage the exploration activities by optimizing the fieldworks, and consequently, the time and cost of the operation. These models can be used in the future mine design and mine planning if they are geometrically accurate. The 3D photogrammetric products such as the point-clouds, mesh models, and digital elevation models (DEM) are directly obtained during the photogrammetric processing. The mesh model and DEM were produced from the dense-point cloud in the Agisoft PhotoScan software. DEM was imported to the Datamine software in order to build an empty wireframe. The trace of large fractures and deposit limits were imported to the Datamine software as the vector format and placed on the wireframe. The sub-surface limit was built and added to the wireframe. The primary block model of the quarry was established based on the wireframe. The established block model was used in order to estimate the resource in the deposit sub-zones.

3.4. Fieldwork and laboratory studies

The value of the dimension stones is due to their appearance, physical properties, and potential of producing rectangular blocks of suitable dimensions [29]. Accordingly, rock sampling was done during the geological survey in order to prepare the specimens for the mineralogical, physical, and geo-mechanical studies. The mineralogy was studied by thin section and XRD. The XRF analysis was undertaken to investigate the presence or absence of the valuable metals and compounds. The geo-mechanical properties were examined by several rock mechanics tests. The Brazilian tensile strength (BTS) and point-load strength index (PLSI) were examined using three samples. The average of 4.65 and 3.91 MPa was estimated for BTS and PLSI, respectively. Due to the rough topography of the quarry, a limited terrestrial fracturing survey was performed through a scan-line parallel to the quarry face. The dominating fracture set exhibited an average dip and dip direction of 70/195.

4. Results and Discussion

4.1. Geological and structural mapping

The exploitability of the dimension stones is controlled by the structural features such as discontinuities, faults, and fractures. A terrestrial fracturing survey is a common approach to determine the specifications of fractures, zones of significant weakness, and geometry of the rock blocks. The Emperador marble quarry represents a rough topography that prevents a complete geological surveying and terrestrial mapping. The geological and fracturing surveys thus are limited to safe places where the topography allows measurements. In such a circumstance, the drones could offer a particular solution to overcome the difficulties of gathering the geological and structural information. The spatial resolution of the acquired images is a decisive parameter for outlining the boundary of geological units and specifying the structural lineaments such as the faults and fractures. Hence, the flight must be conducted at an appropriate altitude in order to ensure the desired spatial resolution.

The flight was performed by DJI Phantom 4 Pro V2.0. A total of 328 images were captured at an altitude of 70 m using the original in-built CMOS camera (effective pixels: 20M). By implementing the Siemens star target, a ground resolution of 3.08 cm/pix was calculated for the 2D photogrammetric products i.e. orthophoto image. Figure 6a shows the orthophoto (orthomosaic) image of the studied area. The orthophoto image was visually interpreted to produce the geology map of the studied area (Figure 3).

In order to facilitate evaluating the resource, the supposed deposit is usually divided into several geological or structural zones. Separating the deposit into several parts can also aid project management by prioritizing the exploration areas. Marble is the only dimension stone in the studied area. Therefore, the deposit was structurally separated considering the structural features. The high-resolution orthophoto image and hill-shade model were used for extracting the fractures across the deposit. Figure 6a displays the enhanced fractures on the deposit surface. The deposit was partitioned into five zones, namely A, B, C, D, and E, considering the location of large fractures. The density of fractures is one of the structural specifications that defines the exploitability of dimension stones [29, 30]. Due to the lack of core samples in the studied area, the surficial density map of fractures was created in order to specify the zones of severe weakness (Figure 6b). The density map is appropriate for determining the surficial variation of the fractures and recognizing the favorable zones. Thus the priority of structural zones can be defined for developing the exploration activities. In the next steps of the exploration work, the fracture densities should be evaluated by modeling the fractures in the 3D space after conducting core drilling. Based on Figure 6b, the zones A, B, and D exhibit a low fracture density, while zone C shows high-density anomalies. The low density of the fractures in zone E is due to the lack of rock outcrops. The rock outcrops in zone E have mainly been covered by *in situ* or placer sediments. According to the defined zones, the strike of fractures was determined using the rose diagrams. All the rose diagrams remarked a major fracture set with an N5E strike (Figure 6C).

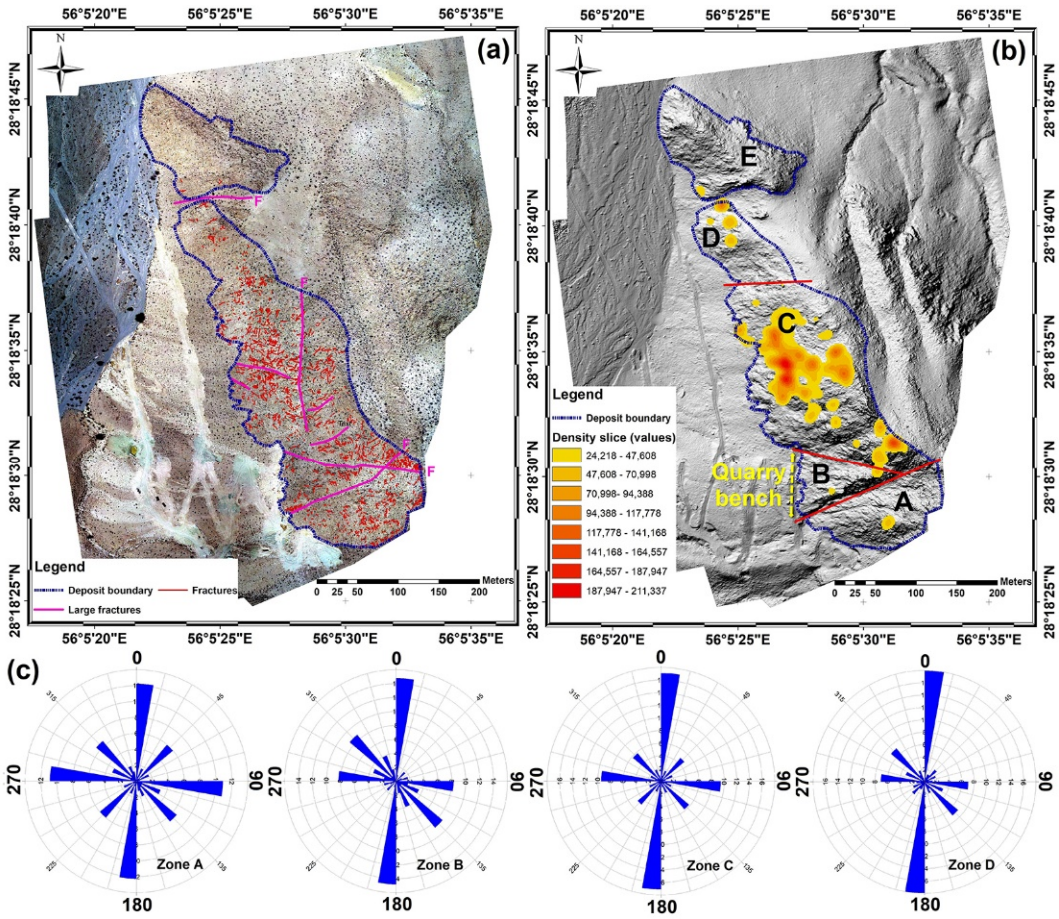

Figure 6. (a) Orthophoto image showing distribution of fractures, (b) hill-shade model and density map of fractures, and (c) rose diagram of different zones annotated on Figure 6b (except zone E due to lack of outcrops).

4.2. 3D deposit modeling

The geological block models are widely used as a basis for the engineering design and production management of mines. Block models are developed at the end of the exploration campaign for estimating the ore deposit and conducting the feasibility studies. If the deposit can structurally or geologically be divided into several zones, the individual block models can be created. In the case of marble stone deposits, where no ore grade is defined, reserve estimation is performed based on the quality indicators [31, 32]. Quality can be defined as the visual or physical aspects such as color, texture, and fractures [31]. All the quality parameters are examined through the performing geological surveys, logging the drillhole samples, and surveying the quarry faces, and can be employed for reconstructing the block model [31]. Finally, the reserve estimation can be done using the geo-statistical analysis [32].

The exploration activities in the Emperador marble quarry involve a limited geological survey and a small quarry bench. No drillhole was available, and the variation of the quality parameters was unknown. Thanks to the highly accurate 3D photogrammetric products, reconstructing a primary block model was undertaken in order to predict the resource largeness of five structural zones. The amount of resources and the situation of fracture densities (Figure 6b) are two factors for selecting the favorable zones for developing fieldwork. This knowledge results in better managing the project to save time and cost. This idea is practical in the beginning steps of an exploration campaign of non-metallic surficial deposits during a high-reliable cost-effective procedure when using the drone imagery. The drone-based photogrammetry can satisfy this task quickly with a low operating cost. In this work, a high-accurate 3D deposit model of the Emperador marble quarry was developed in order to create a primary block model in the initial steps of the mineral exploration program. High accuracy of the primary block model enables

generating an economic block model in the quarry planning stage.

4.2.1. Accuracy assessment of 3D models

Drone-based photogrammetry has facilitated reconstructing the 3D models for the deposits and open-cut mines in the recent years [16, 33-36]. The final products of photogrammetric processing i.e. dense-point cloud, mesh model, and DEM are 3D data that could be upgraded to reconstruct the 3D geological models or block the models of deposits. Thus the geometric accuracy of the 3D models is a concern from the mine designing and planning viewpoint. In this research work, 70% side and 80% front overlap combined with 18 GCPs were considered to ensure the desired accuracy. Figure 7a displays the distribution of GCPs in an area of 0.27 km^2. In order to evaluate the geometric accuracy, four check-points were employed. Table 1 presents the root mean square errors (RMSE) of GCPs. The RMSE of 3.14 was estimated for the check-points (Table 1). Figure 7b shows the reconstructed DEM of the Emperador marble quarry with a resolution of 12.3 cm/pix.

Table 1. RMSE of GCPs and Checkpoints (X - Easting, Y - Northing, Z – Altitude).

Point type	Count	X error (cm)	Y error (cm)	Z error (cm)	Total (cm)
GCP	18	1.60	1.01	2.10	2.83
Check point	4	0.84	2.02	2.26	3.14

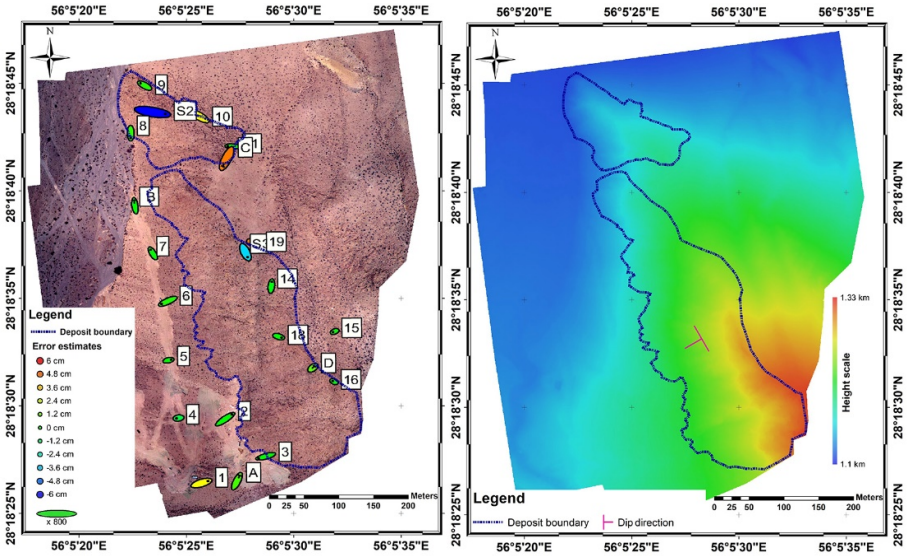

Figure 7. (a) Distribution of GCPs and control points, and (b) digital model elevation of studied area.

4.2.2. Reconstructing 3D models

The deposit limits must be defined before reconstructing the 3D deposit model. The surficial boundary of the Emperador marble quarry was derived from the orthophoto image (based on Figure 6a). At depth, the boundary was created by an inclined surface (mean dip and dip direction of 45/240) based on the marble bed specification. The trace of major fractures was marked on the surface of the 3D deposit model (wireframe). The 3D deposit model was established based on the quarry DEM in the Datamine software (Figure 8a). This 3D model was utilized for generating the primary block model of the deposit (Figures 8a and 8b). Block size (6 m height with a cross-section of 3 m length and 2 m width) was specified based on the experience of quarrying in zone B. The block model was separately created for the zones A, B, C, and D. The large fractures presented in Figure 6a were extended to the depth of the block model considering a 2 m buffer. The affected blocks by large fractures were ignored in estimating the resource. The rock density was considered about 2.65 g/cm^3 based on the laboratory report. The amount of resources was estimated at 295740, 377225, 2157187, and 164851 metric tons for the zones A, B, C, and D, respectively. No block model was constructed for zone E due to the overlying sediments. Block size can be customized for each structural zone according to the quarry testing at the final stages of the exploration campaign.

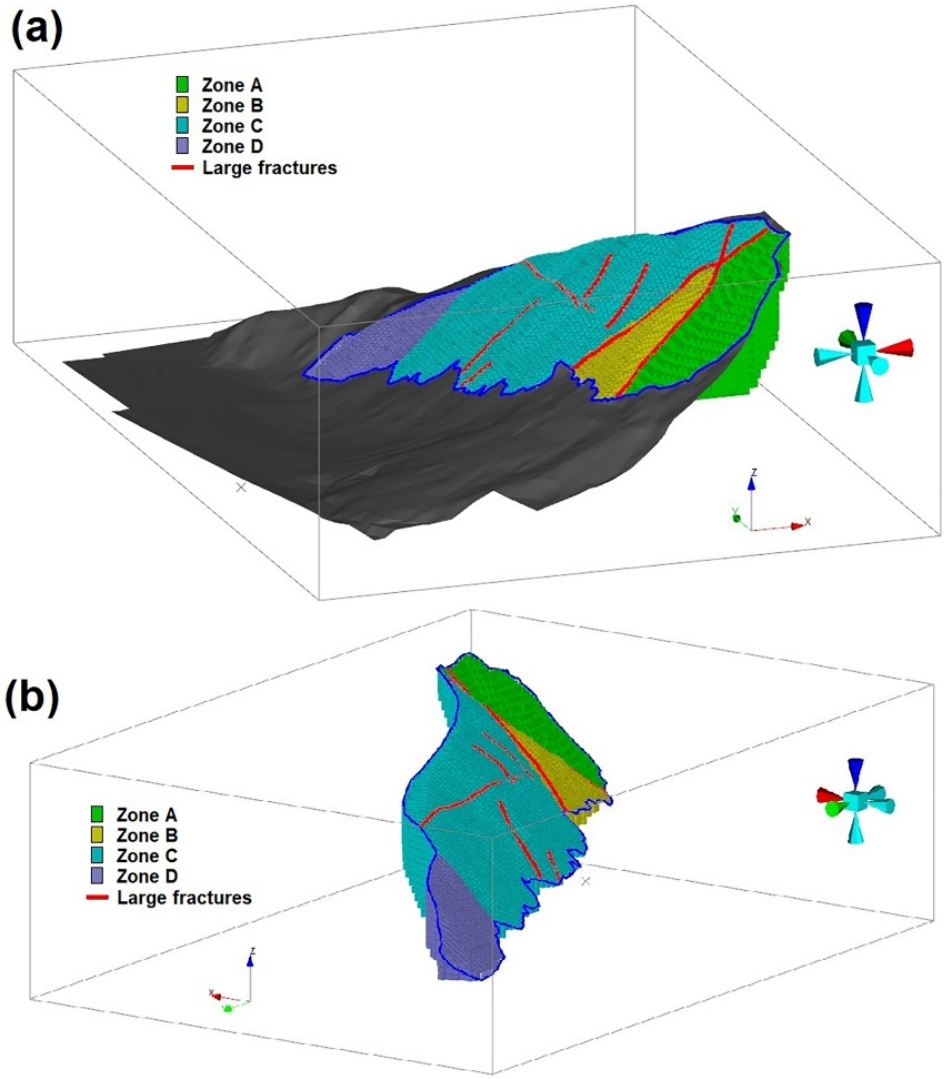

Figure 8. (a) 3D deposit model (wireframe) containing block model, and (b) block model of the Emperador marble quarry.

4.3. Exploration guidelines

In this research work, the drone-based data was suggested to direct fieldwork and re-organize the operation. Using the drone-based data, a new scheme was planned for directing the exploration activities in the studied area. A routine workflow for the exploration of dimension stones can be defined as the desktop study, field investigation, detailed mapping, geophysics, core drilling, reserve evaluation, quarry testing, and test processing [29, 37]. Detailed mapping by a high-resolution drone data led to dividing the marble deposit into five structural zones. This approach made it possible to manage the operation based on the prioritization of exploration in the structural zones. The density of fractures according to Figure 6b and the amount of resources were considered as the basis for the implementation of the exploration priority.

Although high-resolution drone imagery assisted the geological and structural mapping, more information must be collected about the marble bed geometry, appearance (color and texture) uniformity, presence or absence of discontinuities, etc. across the deposit. Thus a detailed geological and fracturing survey must be combined with information derived from boreholes and quarry testing. The non-destructive approaches such as geo-physical methods are preferred before conducting exploratory core drilling and opening the quarry, especially in the regions with environmental consideration. The Emperador marble quarry is located in a semi-arid region,

where the government imposes strict environmental regulations on the mining activities. Therefore, prospectors make special efforts to minimize surface degradation.

Despite the enormous resource of zone C, the zones A and B were chosen as the top priority for developing the exploration activity due to less fracture density considering Figure 6b. The exploration activity should continue through terrestrial fracturing surveys in the zones A and B. Evaluating the status of fractures is necessary for zone A since the relevant rose diagram shows two perpendicular fracture sets (Figure 7C). Then core drilling must be undertaken to assess the situation of fractures, appearance, and thickness at depth. It is recommended to stop quarrying at zone B until completing the fracturing survey. Quarrying can be restarted after receiving promising results from core drilling. Since the quarry testing determines the actual block size, the block model can be revised to increase confidence in estimating the reserve.

The highest fracture density belongs to zone C, where several large fractures have intersected the deposit. This zone is placed in the second-order for developing exploratory works due to the larger resource. Due to the high density of fractures, it is recommended to conduct a geo-radar survey (ground penetrating radar-GPR) before core drilling. Provided that the core drilling indicates an acceptable result, the current quarry face can extend from zone B towards zone C to perform test quarrying (Figures 6a and 6b).

Zone D is located in the third-order because marble outcrops are buried by sediments in some parts. The result of the aerial fracturing survey (Figure 6b) could not convince us to undertake core drilling. A more geological survey is suggested before making any decision. A terrestrial fracturing survey must be done on the marble outcrops, and the thickness of sediments must be determined. Zone E, which was considered in the last, requires more field investigation. Large parts of the zone have been covered by *in situ* and placer sediments. It is essential to measure the thickness of the overburden. A combination of the core drilling and GPR techniques is recommended to evaluate the resource of zone E.

5. Conclusions

The Emperador marble quarry was surveyed using a lightweight commercial drone at the beginning of the mineral exploration program. The main objectives were defined as directing the activities based on the analysis of the drone-based data and predicting the amount of resource before entering the detail phase of exploration. The study of structures and discontinuities in dimension quarries is a vital task but maybe actually limited by rugged topography. Drones have the potential of producing high-resolution 2D products such as orthophoto images, which is appropriate for geological and structural mapping. The spatial resolution is affected by the sensor resolution and the flight altitude. A fight altitude of 70 m is recommended to reach a ground resolution of about 3 cm/pix. This resolution satisfies the geological and structural mapping of the dimension stones.

Preparing a precise geology map is vital for the dimension stone exploration. The geology map can be prepared through the visual interpretation of the orthophoto image. A high-resolution orthophoto image assists in specifying the geological units and defining the deposit boundary even in the inaccessible parts. Dividing the deposit into smaller structural or geological zones enables optimizing the operation by prioritizing the exploratory targets. This approach increases the chances of exploratory success. High-resolution orthophoto image and hill-shade model is suggested for structural mapping. The fractures can be extracted from the orthophoto and hill-shade model, and the density map of fractures should be created. Accordingly, a dimension stone deposit can be divided into several structural zones considering the location of large fractures. Then the structural zones can be prioritized based on the density of fractures, and appropriate methods can be implemented. This procedure helps manage the project, and direct the activities in order to increase the chance of exploration success and decrease the operation cost.

High-accurate 3D products such as mesh models and DEMs are favorites for reconstructing the 3D deposit models. The model comprises the deposit limits and significant structural features. The accuracy level permits using the 3D deposit model for creating the block model in the final stage of the mineral exploration program. The main concern may be the promised accuracy of the 3D model, which is influenced by the flight parameters. This work showed that an accuracy of about 3 cm could be achieved by implementing 80% front and 70% side image overlap. It is recommended to use a grid of GCPs to maximize accuracy. In this research work, a primary block model was reconstructed in order to estimate the marble resource. Having information on the amount of the resource (estimated using the primary block model) along

with the status of fractures can assist in prioritizing the areas under exploration. The research results showed the efficiency of drones in carrying out and managing the exploratory project of surficial dimension stones.

Acknowledgments

We gratefully acknowledge the Surgan Parseh Consulting Engineers (SPCE) for providing the logistics for field visits and sample collections.

References

[1]. Szentpeteri, K., Setiawan, T., and Ismanto, A. (2016). Drones (UAVs) in mining and Exploration. An application example: Pit Mapping and Geological Modelling. Unconventional Exploration Target and new tools in mineral and coal exploration, 45-49.

[2]. Kirsch, M., Lorenz, S., Zimmermann, R., Tusa, L., Möckel, R., Hödl, P., Booysen, R., Khodadadzadeh, M., and Gloaguen, R. (2018). Integration of terrestrial and drone-borne hyperspectral and photogrammetric sensing methods for exploration mapping and mining monitoring. Remote Sensing 10 (9), 1366. doi: 10.3390/rs10091366.

[3]. Carabassa, V., Montero, P., Crespo, M., Padró, J.C., Balagué, J., Alcañiz, J.M., Brotons, L., and Pons, X. (2019). UAS remote sensing products for supporting extraction management and restoration monitoring in open-pit mines. Multi-disciplinary Digital Publishing Institute Proceedings 30 (1), 4. doi:10.3390/proceedings2019030004.

[4]. Shahmoradi, J., Talebi, E., Roghanchi, P., and Hassanalian, M. (2020). A comprehensive review of applications of drone technology in the mining industry. Drones 4 (3), 34. doi: 10.3390/drones4030034.

[5]. Park, S. and Choi, Y. (2020). Applications of unmanned aerial vehicles in mining from exploration to reclamation: A review. Minerals 10 (8), 663. doi: 10.3390/min10080663.

[6]. Blistan, P., Kovanič, Ľ., Zelizňaková, V., and Palková, J. (2016). Using UAV photogrammetry to document rock outcrops. Acta Montanistica Slovaca 21 (2).

[7]. Parvar, K., Braun, A., Layton-Matthews, D., and Burns, M. (2017). UAV magnetometry for chromite exploration in the Samail ophiolite sequence, Oman. Journal of Unmanned Vehicle Systems 6 (1), 57-69. doi: 10.1139/juvs-2017-0015.

[8]. Malehmir, A., Dynesius, L., Paulusson, K., Paulusson, A., Johansson, H., Bastani, M., ... and Marsden, P. (2017). The potential of rotary-wing UAV-based magnetic surveys for mineral exploration: A case study from central Sweden. The Leading Edge, 36(7), 552-557. doi: 10.1190/tle36070552.1.

[9]. Cunningham, M., Samson, C., Wood, A., and Cook, I. (2018). Aeromagnetic surveying with a rotary-wing unmanned aircraft system: A case study from a zinc deposit in Nash Creek, New Brunswick, Canada. Pure and Applied Geophysics, 175(9), 3145-3158. doi: 10.1007/s00024-017-1736-2.

[10]. Walter, C., Braun, A., and Fotopoulos, G. (2020). High-resolution unmanned aerial vehicle aeromagnetic surveys for mineral exploration targets. Geophysical Prospecting, 68(1-Cost-Effective and Innovative Mineral Exploration Solutions), 334-349. doi: 10.1111/1365-2478.12914.

[11]. Dujoncquoy, E., Masse, P., Nicol, Y., Putra, A.S., Kenter, J., Russo, S., and Dhont, D. (2019). UAV-based 3D outcrop analog models for oil and gas exploration and production. In IGARSS 2019-2019 IEEE International Geoscience and Remote Sensing Symposium, IEEE, July, 6791-6794. doi: 10.1109/IGARSS.2019.8900176.

[12]. Heincke, B., Jackisch, R., Saartenoja, A., Salmirinne, H., Rapp, S., Zimmermann, R., ... and Middleton, M. (2019). Developing multi-sensor drones for geological mapping and mineral exploration: Setup and first results from the MULSEDRO project. GEUS Bulletin, 43. doi:10.34194/GEUSB-201943-03-02.

[13]. Honarmand, M. and Shahriari, H. (2021). Geological Mapping using Drone-based Photogrammetry: An Application for Exploration of Vein-Type Cu Mineralization. Minerals 11 (6), 585. doi:10.3390/min11060585.

[14]. Freire, G.R. and Cota, R.F. (2017). Capture of images in inaccessible areas in an underground mine using an unmanned aerial vehicle. In Proceedings of the First International Conference on Underground Mining Technology. Australian Centre for Geomechanics. 10.36487/ACG_rep/1710_54_Freire

[15]. Jackisch, R., Lorenz, S., Zimmermann, R., Möckel, R., and Gloaguen, R. (2018). Drone-borne hyperspectral monitoring of acid mine drainage: An example from the Sokolov lignite district. Remote sensing, 10(3), 385. doi: 10.3390/rs10030385.

[16]. Gil, M. and Frąckiewicz, P. (2019). Optimization of the location of observation network points in open-pit mining's. GIS Forum.

[17]. Katuruza, M. and Birch, C. (2019). The use of unmanned aircraft system technology for highwall mapping at Isibonelo Colliery, South Africa. Journal of the Southern African Institute of Mining and Metallurgy, 119(3), 291-295. doi: 10.17159/2411-9717/2019/v119n3a8.

[18]. Padró, J.C., Muñoz, F.J., Planas, J., and Pons, X. (2019). Comparison of four UAV geo-referencing methods for environmental monitoring purposes focusing on the combined use with airborne and satellite remote sensing platforms. International journal of

applied earth observation and geoinformation, 75, 130-140. doi: 10.1016/j.jag.2018.10.018.

[19]. Mohajjel, M., Fergusson, C.L., and Sahandi, M.R. (2003). Cretaceous–Tertiary convergence and continental collision, Sanandaj–Sirjan zone, western Iran. Journal of Asian Earth Sciences, 21(4), 397-412. doi: 10.1016/S1367-9120(02)00035-4.

[20]. Berberian, M. (1977). Three phases of metamorphism in Haji-Abad quadrangle (southern extremity of the Sanandaj-Sirjan structural zone): a palaeotectonic discussion. Contribution to the Seismotectonics of Iran 239-263.

[21]. Eftekharnejad, J. (1981). Tectonic division of Iran with respect to sedimentary basins. Journal of Iranian Petroleum Society 82, 19–28 (in Farsi).

[22]. Ghasemi, A. and Talbot, C.J. (2006). A new tectonic scenario for the Sanandaj–Sirjan Zone (Iran). Journal of Asian Earth Sciences 26 (6), 683-693. doi: 10.1016/j.jseaes.2005.01.003.

[23]. GSI (1996). Geology Map of Orzuieh (Dashtvar), 1:100000. Tehran: Geological Survey of Iran.

[24]. Dai, J., Xue, L., Sang, X., Li, Z., Ma, J., and Sun, H. (2020, August). Research Method for Dyke Swarms based on UAV Remote Sensing in Desert Areas: A Case Study in Beishan, Gansu, China. In IOP Conference Series: Earth and Environmental Science (Vol. 558, No. 3, p. 032040). IOP Publishing.

[25]. Loebich, C., Wueller, D., Klingen, B., and Jaeger, A. (2007, February). Digital camera resolution measurements using sinusoidal Siemens stars. In Digital Photography III (Vol. 6502, p. 65020N). International Society for Optics and Photonics. doi: 10.1117/12.703817.

[26]. Honkavaara, E., Peltoniemi, J., Ahokas, E., Kuittinen, R., Hyyppa, J., Jaakkola, J., ... and Suomalainen, J. (2008). A permanent test field for digital photogrammetric systems. Photogrammetric engineering and remote sensing, 74(1).

[27]. Orych, A. (2015). Review of methods for determining the spatial resolution of UAV sensors. International Archives of the Photogrammetry, Remote Sensing and Spatial Information Sciences 40. doi: 10.5194/isprsarchives-XL-1-W4-391-2015.

[28]. Stöcker, C., Nex, F.C., Koeva, M.N., and Zevenbergen, J.A. (2018). Data quality assessment of UAV-based products for land tenure recording in East Africa. In NCG symposium 2018.)

[29]. Ashmole, I. and Motloung, M. (2008). Dimension stone: the latest trends in exploration and production technology. In Proceedings of the International Conference on Surface Mining 5, 8.

[30]. Taboada, J., Rivas, T., Saavedra, A., Ordóñez, C., Bastante, F., and Giráldez, E. (2008). Evaluation of the reserve of a granite deposit by fuzzy kriging. Engineering Geology, 99(1-2), 23-30. doi:10.1016/j.enggeo.2008.02.001.

[31]. Kapageridis, I. and Albanopoulos, C. (2016). Reserves estimation of a marble quarry using quality indicators. Bulletin of the Geological Society of Greece, 50(4), 1849-1858. doi: 10.12681/bgsg.11924.

[32]. Exadaktylos, G. and Saratsis, G. (2020). Methodology for the Estimation and classification of white marble reserves. Mining, Metallurgy and Exploration, 37(4), 981-994. doi: 10.1007/s42461-020-00228-3.

[33]. Wang, Q., Wu, L., Chen, S., Shu, D., Xu, Z., Li, F., and Wang, R. (2014). Accuracy evaluation of 3D geometry from low-attitude UAV images: a case study at Zijin mine. International Archives of the Photogrammetry, Remote Sensing and Spatial Information Sciences, 4.

[34]. Chirico, P.G. and DeWitt, J.D. (2017). Mapping informal small-scale mining features in a data-sparse tropical environment with a small UAS. Journal of Unmanned Vehicle Systems, 5(3), 69-91. doi: 10.1139/juvs-2017-0002

[35]. Rossi, P., Mancini, F., Dubbini, M., Mazzone, F., and Capra, A. (2017). Combining nadir and oblique UAV imagery to reconstruct quarry topography: methodology and feasibility analysis. European Journal of Remote Sensing, 50(1), 211-221.

[36]. Madjid, M.Y.A., Vandeginste, V., Hampson, G., Jordan, C.J., and Booth, A.D. (2018). Drones in carbonate geology: Opportunities and challenges, and application in diagenetic dolomite geo-body mapping. Marine and Petroleum Geology, 91, 723-734. doi: 10.1016/j.marpetgeo.2018.02.002.

[37]. Luodes, H., Selonen, O., and Pääkkönen, K. (2000). Evaluation of dimension stone in gneissic rocks-a case history from southern Finland. Engineering Geology, 58(2), 209-223. doi: 10.1016/S0013-7952(00)00059-4.

کاربرد داده های مبتنی بر پهپاد برای هدایت فعالیت‌های اکتشافی و تخمین منابع در معدن سنگ مرمریت امپرادور، استان کرمان، ایران

هادی شهریاری[1*]، مهدی هنرمند[2]، سعید میرزائی[3] و امیر صفاری[4و5]

۱- گروه مهندسی معدن، دانشکده فنی و مهندسی، دانشگاه ولی عصر (عج) رفسنجان، رفسنجان، ایران

۲- گروه اکولوژی، پژوهشگاه علوم و تکنولوژی پیشرفته و علوم محیطی، دانشگاه تحصیلات تکمیلی صنعتی و فناوری پیشرفته، کرمان، ایران

۳- گروه مهندسی معدن، معدن مس سرچشمه، شرکت ملی صنایع مس ایران، ایران

۴- دانشکده مهندسی معدن، نفت و ژئوفیزیک، دانشگاه صنعتی شاهرود، شاهرود، ایران

۵- دفتر فنی، شرکت زغال سنگ البرز شرقی، شاهرود، ایران

ارسال ۲۰۲۲/۰۱/۳۱، پذیرش ۲۰۲۲/۰۲/۲۴

* نویسنده مسئول مکاتبات: shahriarihi@gmail.com

چکیده:

این کار تحقیقاتی در نظر دارد روش استفاده از داده‌های پهپاد در مراحل اولیه برنامه اکتشاف ذخایر سنگ نما را مورد بحث قرار دهد. یک تصویربرداری با وضوح بالا توسط پهپاد تجاری ارزان قیمت در معدن سنگ مرمر امپرادور، استان کرمان، ایران انجام می‌شود. قدرت تفکیک زمینی ۳ سانتی‌متر بر پیکسل با تصویربرداری در ارتفاع ۷۰ متری به منظور اطمینان از نقشه‌برداری سنگ‌شناسی و ساختاری دقیق به دست می‌آید. دقتی کمتر از ۵ سانتی متر برای محصولات فتوگرامتری سه بعدی بر عهده گرفته می‌شود. از این رو، پرواز با ۸۰ درصد و ۷۰ درصد همپوشانی طولی و جانبی تصویر انجام می‌گردد. علاوه بر این، ۱۸ نقطه کنترل زمینی (GCPs) به منظور دستیابی به دقت مورد نیاز استفاده می‌شود. پردازش فتوگرامتری توسط نرم افزار Agisoft PhotoScan انجام می‌پذیرد. نقشه زمین شناسی از طریق تفسیر بصری تصویر ارتوفتو تهیه می‌گردد. گسل ها و شکستگی ها با استفاده از مدل ارتوفتو و سایه-روشن با وضوح بالا در نرم افزار ArcGIS ترسیم می‌شوند. بر این اساس، نقشه تراکم شکستگی ها تهیه و کانسار به پنج ناحیه ساختاری تقسیم می‌شود. مدل سه بعدی کانسار با دقت ۲/۸ سانتی متر بر اساس مدل ارتفاعی رقومی (DEM) باز سازی می‌گردد. یک مدل بلوکی اولیه با استفاده از مدل سه بعدی کانسار در نرم افزار Datamine به منظور تخمین منبع برای هر منطقه ساختاری تولید می‌شود. در نهایت با توجه به میزان منبع و وضعیت شکستگی ها، اولویت اکتشاف برای توسعه فعالیت‌ها و روش‌های مناسب برای هر ناحیه ساختاری تعریف می‌گردد. نتایج کار تحقیقاتی، ما را متقاعد می‌سازد به منظور صرفه جویی در زمان و هزینه عملیات، تصویربرداری پهپادی را در مراحل اولیه اکتشاف سنگ‌های نما بگنجانیم.

کلمات کلیدی: تصویربرداری پهپادی، فتوگرامتری، معدن سنگ مرمریت، مدل سه بعدی کانسار، مدل بلوکی، تخمین ذخیره.